

in such cases are restricted^{15,18} to ${}_4T^3$ or to a small range⁴ of conformations, ${}_4T^3 \leftrightarrow {}^3T_4$. The pseudorotation parameter, P , of initially known structures fell into a narrow range (37–48°). However, in Table III it is seen that the phase angles (P) can have values over a much wider range (15–57°).

The six-membered phosphate rings are in the chair conformation and are slightly flattened at the phosphate end, probably because the P–O bonds are longer than the other bonds in the ring.

Hydrogen Bonding and Dimer Formation. A striking feature of the structure is the formation of the dimer seen in Figure 2. The two molecules are oriented in an antiparallel fashion and O(2') of molecule A is hydrogen bonded to N(3) of molecule B with an H...N distance of 1.73 Å. The O(2') of B is in turn hydrogen bonded to N(3) of A with an H...N distance of 1.91 Å. Hydrogen-bond parameters are listed in Table V. The phosphate oxygens are heavily hydrated, and O(7A) accepts three hydrogen bonds from water molecules while O(7B) is an acceptor for two hydrogen bonds. In both molecules, N(6) has only one hydrogen bond.

Sodium Coordination. Na(1) is octahedrally coordinated to five water molecules and O(6A), with coordination distances varying

from 2.377 to 2.454 Å. The number of angles made by the six coordinating atoms at the central ion is 15, and in a regular octahedron, 12 of these are 90° and 3 are 180°. At Na(1) the maximum deviation from these ideal values is 21°. For Na(2) the coordination distances vary from 2.354 to 2.734 Å and for the angles the maximum deviation from the ideal values is 51°, which indicates a much larger deviation from ideal octahedral geometry. This deviation may reflect the fact that, while for Na(1), 5 of the coordinating atoms are water oxygens, in the case of the Na(2) atom three of the coordinating oxygens belong to water molecules and the other three are parts of the cAMP molecule.

Acknowledgment. We thank the New York State Department of Health and the National Institute of Health (Grants GM 22490 and CA 23597) for support.

Registry No. CAMP, Na, 33116-15-3.

Supplementary Material Available: Listing of the structure factor amplitudes and anisotropic thermal parameters and a table giving the coordination geometry around sodium ions (18 pages). Ordering information is given on any current masthead page.

Crystal and Molecular Structure of the Quinoxaline Antibiotic Analogue TANDEM (Des-*N*-tetramethyltrioistin A)

M. B. Hossain,^{1a} Dick van der Helm,^{*1a} Richard K. Olsen,^{1b} Peter G. Jones,^{1c} George M. Sheldrick,^{1c} Ernst Egert,^{1d} Olga Kennard,^{1d} Michael J. Waring,^{1e} and M. A. Viswamitra^{1f}

Contribution from the Department of Chemistry, Oklahoma University, Norman, Oklahoma 73019, Department of Chemistry and Biochemistry, Utah State University, Logan, Utah, Anorganisch-Chemisches Institut, University of Göttingen, Federal Republic of Germany, University Chemical Laboratory, Cambridge, United Kingdom, Department of Pharmacology, University of Cambridge, Cambridge, United Kingdom, and Indian Institute of Science, Bangalore, India. Received July 9, 1981

Abstract: The crystal structure of TANDEM (des-*N*-tetramethyltrioistin A), a synthetic analogue of the quinoxaline antibiotic trioistin A, has been determined independently at –135 and 7 °C and refined to R values of 0.088 and 0.147, respectively. The molecule has approximate 2-fold symmetry, with the quinoxaline chromophores and the disulfide cross-bridge projecting from opposite sides of the peptide ring. The quinoxaline groups are nearly parallel to each other and separated by about 6.5 Å. The peptide backbone resembles a distorted antiparallel β ribbon joined by intramolecular hydrogen bonds N–H(L-Val)–O(L-Ala). At low temperatures, the TANDEM molecule is surrounded by a regular first- and second-order hydration sphere containing 14 independent water molecules. At room temperature, only the first-order hydration shell is maintained. Calculations of the interplanar separation of the quinoxaline groups as a function of their orientation with respect to the peptide ring support the viability of TANDEM to intercalate bifunctionally into DNA.

Des-*N*-tetramethyltrioistin A (TANDEM), a synthetic analogue in the trioistin family of quinoxaline antibiotics, was synthesized by Ciardelli, Chakravarty, and Olsen.^{2a} The natural antibiotic, trioistin A,^{2b} is a symmetrical bicyclic octadepsipeptide composed of two units each of D-serine, L-alanine, *N*-methyl-L-cysteine, and *N*-methyl-L-valine. The depsipeptide bond occurs between the

hydroxyl group of D-serine and the carboxyl group of *N*-methyl-L-valine, while a disulfide cross-bridge connects the two *N*-methyl-L-cysteine units. A 2-quinoxaline carbonyl (Qxc) moiety is attached to the amino group of each D-Ser unit. The title compound (Figure 1) differs from trioistin A by the lack of *N*-methyl groups on the L-Cys and L-Val residues.

The quinoxaline antibiotics are active against Gram-positive bacteria³ and against certain animal tumors.⁴ The trioistin an-

(1) (a) Oklahoma University; (b) Utah State University; (c) University of Göttingen; (d) University Chemical Laboratory, Cambridge; (e) University of Cambridge; (f) Indian Institute of Science.

(2) (a) Ciardelli, T. L.; Chakravarty, P. K.; Olsen, R. K. *J. Am. Chem. Soc.* **1978**, *100*, 7684–7690. (b) Otsuka, H.; Shōji, J. *Tetrahedron* **1967**, *23*, 1535–1542. Otsuka, H.; Shōji, J.; Kawano, K.; Kyogoku, Y. *J. Antibiot.* **1976**, *29*, 107–110. Chakravarty, P. K.; Olsen, R. K. *Tetrahedron Lett.* **1978**, 1613–1616.

(3) Shōji, J.; Katagiri, K. *J. Antibiot., Ser. A* **1961**, *14*, 335–339. Katagiri, K.; Yoshida, T.; Sato, K. "Antibiotics III. Mechanism of Action of Antimicrobial and Antitumor Agents"; Corcoran, J. W., Hahn, F. E., Eds.; Springer-Verlag: New York, 1975; pp 234–251.

(4) Matsuura, S. *J. Antibiot., Ser. A* **1965**, *18*, 43–46.

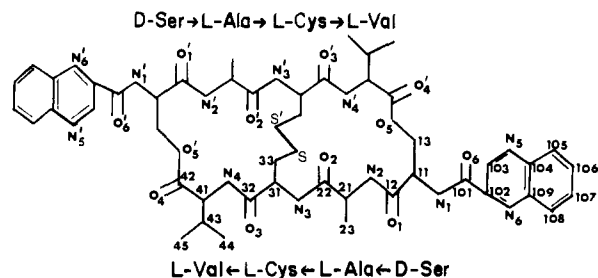


Figure 1. A schematic drawing of TANDEM showing the atom numbering. The molecule is divided into two parts, primed and unprimed, related by 2-fold symmetry.

tibiotics have been shown to bind strongly to double-stranded DNA⁵ and thereby function as potent inhibitors of RNA synthesis.⁶ The mode of binding of these antibiotics is known to be bifunctional intercalation in which both the quinoxaline rings have undergone simultaneous intercalation. The recently discovered quinoline-containing group of antibiotics, designated as **BBM-928**,⁷ are quite similar to the quinoxaline antibiotics.

From an extensive study of the interaction between TANDEM and nucleic acids, Lee and Waring concluded that the mechanism of DNA binding for this compound involves bifunctional intercalation similar to that seen with other members of the triostin family. Among several synthetic triostin derivatives, the binding constant is highest for TANDEM.⁸ They also showed that TANDEM displays a strong preference for (A + T)-rich DNA species, with the highest binding constant for poly(dA-dT). It is suggested that this antibiotic analogue binds to double-stranded DNA via its minor groove and possibly forms a two-base-pair sandwich.

The molecular structure and conformation of several quinoxaline antibiotics, including echinomycin⁹ and triostin A,¹⁰ have been investigated in solution. Both in echinomycin and triostin A, the proposed model has a rigid peptide ring with parallel chromophores extending roughly perpendicular to the mean plane of the peptide ring with space between the chromophores sufficient to accommodate two DNA base pairs. Triostin A exists in two different conformers, both of which appear to retain 2-fold symmetry in solution. It has been suggested⁸ that the conformation of TANDEM may differ from that of triostin A with regard to the disposition of the S-S cross-bridge, which might lie on the same side as the chromophores in TANDEM but be free to move to either side in the natural antibiotic.

The crystal structure determination of TANDEM was undertaken with the expectation that this might lead to a better understanding of its mode of binding to DNA. The structure was simultaneously and independently solved by two groups. While one (Oklahoma) worked with low-temperature data collected at 138 K (referred to in the text as the LT structure), the group at Cambridge (U.K.) used 280 K data (referred to as the RT structure). Because some significant conformational differences

(5) Lee, J. S.; Waring, M. J. *Biochem. J.* **1978**, *173*, 115-128. M. J. Waring "Antibiotics V/Part 2. Mechanism of Action of Antileukaryotic and Antiviral Compounds"; Hahn, F. E., Ed.; Springer-Verlag: New York, 1979; pp 173-194.

(6) Waring, M. J.; Makoff, A. *Mol. Pharmacol.* **1974**, *10*, 214-224. Gause, G. G., Jr.; Loshkareva, N. P.; Zbarsky, I. B. *Biochim. Biophys. Acta* **1968**, *166*, 752-754.

(7) Ohkuma, H.; Sakai, F.; Nishiyama, Y.; Ohbayashi, M.; Imanishi, H.; Konishi, M.; Mlayaki, T.; Koshiyama, H.; Kawaguchi, H. *J. Antibiot.* **1980**, *33*, 1087-1097. Tomita, K.; Hoshino, Y.; Sasahira, T.; Kawaguchi, H. *Ibid.* **1980**, *33*, 1098-1102. Huang, C-H; Mong, S.; Crooke, S. T. *Biochemistry* **1980**, *19*, 5537-5542. Konishi, M.; Ohkuma, H.; Sakai, F.; Tsuno, T.; Koshiyama, H.; Naito, T.; Kawaguchi, H. *J. Antibiot.* **1981**, *34*, 148-159. Konishi, M.; Ohkuma, H.; Sakai, F.; Tsuno, T.; Koshiyama, H.; Naito, T.; Kawaguchi, H. *J. Am. Chem. Soc.* **1981**, *103*, 1241-1243. Arnold, E.; Clardy, J. *Ibid.* **1981**, *103*, 1243-1244.

(8) Lee, J. S.; Waring, M. J. *Biochem. J.* **1978**, *173*, 129-144 and references therein.

(9) Cheung, H. T.; Feeney, J.; Roberts, G. C. K.; Williams, D. H.; Ughetto, G.; Waring, M. J. *J. Am. Chem. Soc.* **1978**, *100*, 46-54.

(10) Kalman, J. R.; Blake, T. J.; Williams, D. H.; Feeney, J.; Roberts, G. C. K. *J. Chem. Soc., Perkin Trans I* **1979**, 1313-1321.

Table I. Crystal Data

	LT structure	RT structure
mol formula	C ₄₆ H ₅₄ N ₁₂ O ₁₂ S ₂ · 12H ₂ O	C ₄₆ H ₅₄ N ₁₂ O ₁₂ S ₂ · 12H ₂ O
mol wt	1283.3	1247.3
cell dimensions	<i>a</i> = 17.989 (5) Å <i>b</i> = 21.793 (4) Å <i>c</i> = 16.153 (10) Å <i>V</i> = 6332.5 Å ³	18.400 (10) Å 22.126 (8) Å 16.435 (6) Å 6691.0 Å ³
space group	<i>P</i> 2 ₁ 2 ₁ 2 ₁	<i>P</i> 2 ₁ 2 ₁ 2 ₁
calcd density, g·cm ⁻³	1.346	1.238
radiation	Cu Kα	Mo Kα
wavelength, Å	1.54178	0.71069
2θ _{max} , deg	150	50
total number of reflections	7162	5455
number of observed reflections (<i>F</i> > 2σ(<i>F</i>))	5192	4111
resolution, Å	0.80	0.85
temp, °C	-135 (2)	7(1)

are observed in the two structure determinations of the TANDEM molecule, the results of both studies are incorporated in the present paper. It should be realized that the structure determinations were at different temperatures and that the compound was crystallized from different solvents.

Experimental Section

LT Structure. Plate-shaped crystals of TANDEM were obtained from a methanol solution equilibrated with water at 0 °C. The crystals were found to be unstable in air but stable at low temperatures. Therefore, a chosen crystal (size: 0.45 × 0.18 × 0.11 mm) was mounted by dipping a greased glass fiber inside the mother liquor. The mounted crystal was then transferred quickly to the diffractometer, where it was immersed in a jet of cold nitrogen vapor at -135 (2) °C. All intensity measurements were carried out at this temperature. From the systematic absences, the space group was determined as *P*2₁2₁2₁. The cell parameters were obtained by a least-squares fit to +2θ and -2θ values of 32 reflections. The crystal data are listed in Table I.

Intensities of all unique reflections with 2θ < 150° were measured by using Ni-filtered Cu Kα radiation (λ = 1.54178 Å) and θ-2θ scan techniques with variable scan rates. The scan angle was calculated for each reflection as (1.0 + 0.1 tan θ)°. A receiving aperture with a variable width of (4.5 + 0.86 tan θ) mm and a constant height of 6 mm was placed at a distance of 173 mm from the crystal. The maximum scan time for a reflection of 75 s, of which two-thirds was spent scanning the peak and one-sixth in measuring each of the two backgrounds. During the data collection, the intensity of a monitor reflection was checked every 50 min. The monitor intensity gradually decreased by 9.5% during the seven days of data collection. In all 7162 independent reflections were measured, out of which 1970 with *I* < 2σ(*I*) were considered unobserved. All intensity data were scaled by means of the monitor intensity. Lorentz and polarization corrections were applied. No absorption correction was made.

RT Structure. Crystals in the form of colorless rectangular blocks were grown from dimethylformamide/ethanol/water. The crystal used for data collection (0.7 × 0.4 × 0.3 mm) was sealed with mother liquor in a capillary to prevent the otherwise rapid decomposition by loss of solvent.

Data were collected at 7 (1) °C on a Stoe two-circle diffractometer using monochromated Mo Kα radiation (λ = 0.71069 Å). Layers 0kl-16kl afforded 5455 reflections in the range 0 < 2θ < 50°; averaging equivalent reflections gave 4111 unique structure factors with *F* > 2σ(*F*).

Structure Determination and Refinement

LT Structure. When early attempts to solve the structure by direct methods programs, MULTAN76 and SHELX, and by three-dimensional Patterson analyses failed, MULTAN78 was tried by changing one or more of the following: (1) the number of *E* values; (2) the contents of the unit cell (unknown because of the presence of a substantial amount of solvent); (3) the number of reflections in the starting set; (4) inclusion of atom groups of known geometry in the calculation of *E* values; (5) exclusion of two very strong high-order reflections (14,7,0 and 15,1,1).

In one of these many runs, a phase set of 600 reflections with *E* > 1.57 led to an *E* map which showed very encouraging signs. It is interesting to note that for this MULTAN attempt sulfur atoms were deliberately left out of the calculations of *E* values. The *E* map contained two large peaks separated by about 2.0 Å and clearly showed the two quinoxaline rings

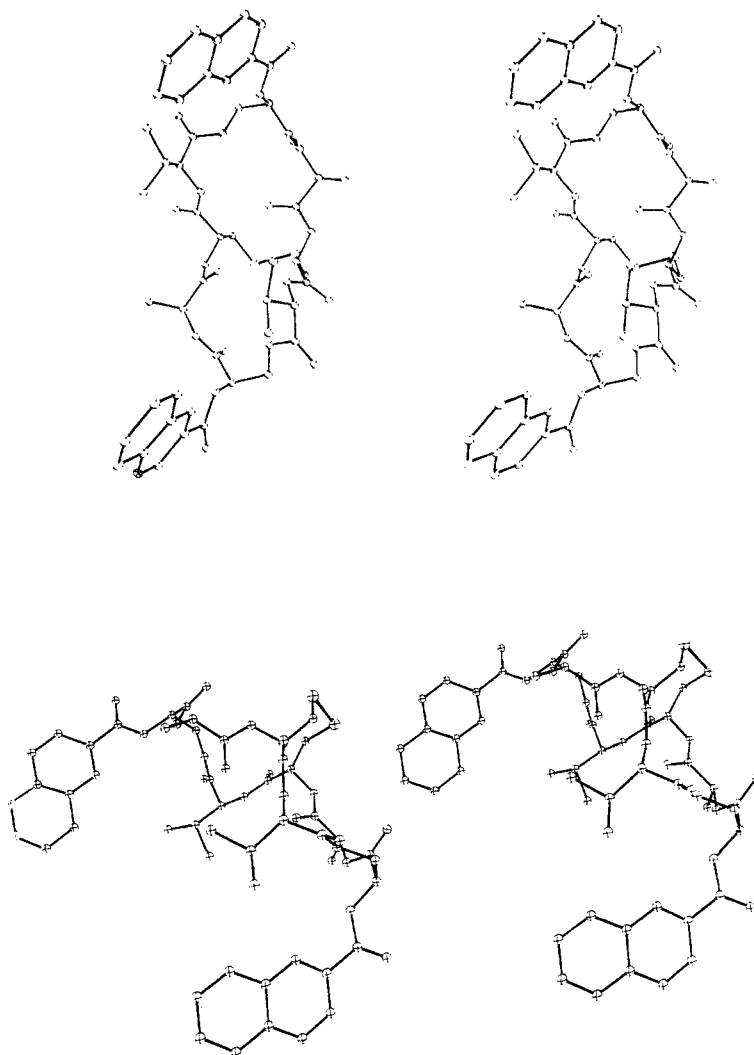


Figure 2. Two stereo views of the TANDEM molecule at LT.

and part of the peptide chain, altogether 46 atoms. Since the tangent formula recycling procedure failed to expand the structure, the partial structure was refined isotropically by a block-diagonal least-squares program using only the 2950 strongest reflections. After three cycles, when the discrepancy factor was reduced to 0.32, a difference Fourier synthesis yielded the missing atoms in the peptide backbone. The rest of the structure including 14 water oxygens, was obtained from successive difference electron-density maps. All the atoms except the solvent atoms were refined with anisotropic thermal parameters. When the R factor for the observed reflections was 0.098, anomalous dispersion effects due to sulfur atoms were taken into account. Attempts to locate hydrogen atoms were only partially successful. It was therefore decided to place 36 H atoms at their calculated positions. They were included in the structure factor calculations, but excluded from refinement. The final R factor was 0.088 for 5013 observed reflections and 0.125 for all 7162 data. The refinement was discontinued when the parameter shifts became insignificant ($\Delta < 1/3\sigma$). Positional parameters are listed in Table II.

RT Structure. The structure was solved with some difficulty by multisolution tangent refinement using a Data General Eclipse mini-computer and the SHELXTL programs written by G.M.S. In one of many attempts, 300 phases were refined and expanded to 692 E values ($E > 1.38$). "Magic integers" were used to assign initial phases to the starting set of 16 reflections. The solution with the best values for both figures of merit (NQUEST and R_α) showed substantial parts of both aromatic systems (as in many other E maps before), but the breakthrough consisted of correctly assigning peaks 1 and 6 (ranked in order of height) to the two sulfur atoms. Partial structure expansion was accelerated by a new E -Fourier recycling procedure in which chemical connectivity considerations were used automatically to decide which peaks to accept as atoms. The first such cycle, in fact, yielded the full structure except for solvent molecules and a few side groups, which appeared in a subsequent difference electron-density synthesis.

The structure was refined by cascade-blocked least-squares methods with all non-hydrogen atoms anisotropic (primarily to accommodate partial disorder introduced by the variable solvent composition of the unit cell). It was necessary to constrain a few U_{ij} to prevent atoms going non-positive-definite. A riding model was employed for hydrogen atoms (C-H = 0.96 Å), with their temperature factors fixed at 1.2 times the equivalent isotropic temperature factors of the atoms to which they were attached. Refinement converged to $R = 0.147$ ($R_w = 0.124$), with $w = \{\omega(F)^2 + 0.0005F^2\}^{-1}$ for 4111 observed data. Eleven low angle reflections were omitted because they were strongly affected by the disordered solvent molecules. It was recognized that the positions of all but four water oxygen atoms were only partially occupied, as reflected in their high thermal parameters (Table II). Other positions of disordered solvent molecules could be located on the final difference map. However, no attempt was made to interpret these.

Results

The final positional and equivalent isotropic thermal parameters are listed in Table II. The atom numbering scheme adopted in the present report is shown in Figure 1. Bond lengths and bond angles are given in Table III and Table IV, respectively. The torsion angles are shown in Figure 3. Values relating to the RT structure are given in parentheses.

A stereo view of TANDEM is shown in Figure 2. The absolute configuration was assumed from the known configurations of the amino acids. The depsipeptide ring is essentially flat and assumes the shape of a slightly twisted disk. The standard deviation of the 26 ring atoms from their mean plane is 0.77 Å (0.69 Å) and the maximum deviation 1.6 Å (1.3 Å). The length of the disk (C(11)–C'(11)) is 11.9 Å (12.2 Å), while its minimum breadth (distance between the L-Cys–C $^\alpha$ atoms) is 3.8 Å (3.9 Å). The

Table II (Continued)

	<i>x</i>	<i>y</i>	<i>z</i>	<i>U</i>		<i>x</i>	<i>y</i>	<i>z</i>	<i>U</i>
W(5)	5158 (4)	-1853 (3)	2163 (5)	445 (25)	W(9)	7315 (4)	1396 (3)	-1495 (4)	394 (25)
	5146 (7)	-1798 (5)	2220 (7)	500 (40)		7495 (5)	1252 (5)	-1489 (7)	390 (40)
W(6)	6320 (4)	-2743 (4)	1968 (5)	508 (25)	W(10)	8976 (4)	-1514 (4)	-2508 (5)	559 (25)
	6726 (10)	-1987 (11)	2356 (10)	1460 (100)		9594 (22)	-1381 (21)	-2919 (16)	3280 (210)
W(7)	6148 (4)	-3852 (4)	-408 (5)	494 (25)	W(11)	-208 (4)	-1255 (4)	-362 (5)	494 (25)
	6587 (23)	-4134 (14)	85 (24)	3380 (200)	W(12)	2137 (4)	-1874 (4)	-618 (5)	533 (25)
W(8)	8201 (4)	-1007 (4)	-360 (5)	546 (25)	W(13)	7727 (4)	-2202 (4)	-438 (5)	584 (25)
	8091 (24)	-1439 (20)	-352 (13)	3550 (210)		8374 (15)	-1546 (14)	-989 (24)	2680 (170)
					W(14)	9213 (5)	-2328 (4)	-1269 (6)	686 (25)
						9542 (16)	-2110 (11)	-1967 (16)	1980 (130)

^a In this table and also in Tables III and IV, the upper values correspond to the LT and the lower values to the RT structure. ^b $U = (1/e^2) \sum_i \sum_j b_i b_j \bar{a}_i \bar{a}_j$. ^c Standard deviations for last digit are listed within parentheses.

Table III. Bond Lengths^a

		primed		primed
S(1)-S'(1)	2.040 (4)		C(41)-C(42)	1.457 (13)
	2.008 (7)			1.506 (15)
S(1)-C(33)	1.816 (10)	1.805 (10)	C(41)-C(43)	1.542 (24)
	1.811 (18)	1.823 (16)		1.508 (22)
N(1)-C(11)	1.482 (11)	1.461 (11)	C(42)-O(4)	1.543 (13)
	1.435 (17)	1.484 (17)		1.548 (13)
C(11)-C(12)	1.541 (14)	1.519 (14)	C(42)-O'(5)	1.642 (32)
	1.536 (24)	1.458 (19)		1.515 (19)
C(11)-C(13)	1.567 (14)	1.559 (14)	C(43)-C(44)	1.239 (12)
	1.564 (19)	1.581 (20)		1.190 (12)
C(13)-O(5)	1.440 (13)	1.446 (11)		1.208 (20)
	1.384 (18)	1.414 (18)	C(43)-C(45)	1.346 (12)
C(12)-O(1)	1.218 (11)	1.256 (11)		1.368 (13)
	1.223 (22)	1.213 (17)	C(43)-C(44)	1.286 (20)
C(12)-N(2)	1.359 (13)	1.335 (12)		1.296 (19)
	1.345 (25)	1.345 (17)	C(43)-C(44)	1.542 (15)
N(2)-C(21)	1.462 (12)	1.458 (12)		1.557 (15)
	1.397 (18)	1.415 (18)	C(43)-C(45)	1.425 (60)
C(21)-C(22)	1.488 (13)	1.559 (13)		1.516 (26)
	1.471 (21)	1.611 (19)	C(43)-C(45)	1.515 (15)
C(21)-C(23)	1.547 (14)	1.513 (14)		1.567 (14)
	1.591 (20)	1.519 (20)	N(1)-C(101)	1.593 (46)
C(22)-O(2)	1.252 (12)	1.203 (11)		1.612 (21)
	1.256 (20)	1.249 (18)	C(101)-C(102)	1.336 (12)
C(22)-N(3)	1.341 (11)	1.358 (12)		1.348 (13)
	1.323 (18)	1.261 (19)	C(101)-O(6)	1.350 (19)
N(3)-C(31)	1.444 (12)	1.460 (12)		1.247 (11)
	1.430 (19)	1.428 (18)	C(101)-C(102)	1.255 (12)
C(31)-C(32)	1.523 (14)	1.518 (13)		1.247 (11)
	1.391 (22)	1.496 (18)	C(101)-C(102)	1.165 (18)
C(31)-C(33)	1.521 (13)	1.503 (14)		1.152 (18)
	1.493 (21)	1.521 (20)	C(101)-C(102)	1.492 (13)
C(32)-O(3)	1.237 (13)	1.230 (12)		1.472 (13)
	1.256 (21)	1.197 (17)	C(102)-C(103)	1.494 (21)
C(32)-N(4)	1.330 (13)	1.356 (12)		1.572 (21)
	1.348 (20)	1.339 (17)	C(102)-C(103)	1.449 (13)
N(4)-C(41)	1.466 (13)	1.439 (12)		1.432 (14)
	1.461 (19)	1.404 (16)	C(103)-N(5)	1.452 (20)
				1.428 (22)
			C(103)-N(5)	1.324 (12)
				1.315 (12)
			N(5)-C(104)	1.349 (17)
				1.249 (21)
			C(104)-C(105)	1.388 (13)
				1.340 (12)
			C(104)-C(105)	1.339 (19)
				1.373 (20)
			C(104)-C(105)	1.384 (13)
				1.393 (12)
			C(104)-C(109)	1.349 (21)
				1.388 (24)
			C(104)-C(109)	1.384 (12)
				1.462 (14)
			C(105)-C(106)	1.387 (22)
				1.414 (24)
			C(105)-C(106)	1.417 (16)
				1.375 (13)
			C(106)-C(107)	1.352 (26)
				1.301 (29)
			C(106)-C(107)	1.401 (14)
				1.418 (15)
			C(107)-C(108)	1.469 (23)
				1.427 (37)
			C(107)-C(108)	1.383 (13)
				1.369 (13)
			C(108)-C(109)	1.377 (24)
				1.441 (15)
			C(108)-C(109)	1.454 (14)
				1.396 (13)
			C(109)-N(6)	1.354 (27)
				1.415 (22)
			C(109)-N(6)	1.336 (12)
				1.335 (11)
			N(6)-C(102)	1.382 (20)
				1.384 (17)
				1.300 (12)
				1.213 (16)
				1.370 (18)

^a Related distances in the "unprimed" and "primed" parts of the molecule (see Figure 1) are listed in parallel columns. Standard deviations are within parentheses.

quinoxaline groups and the valyl side chains lie on one side of the peptide ring ("up"), while the disulfide cross-bridge projects from the other side ("down"). The Qxc moieties are approximately perpendicular to the peptide plane, with angles of 90° and 88° (86° and 84°). The two chromophores are nearly parallel (angle: 7° LT, 14° RT) and separated by about 6.5 Å. The peptide units form a distorted β -pleated structure with all peptide linkages trans. All ω -torsion angles (Figure 3) lie close to 180° (maximum deviation: 7° LT, 11° RT). There are two very weak intramolecular hydrogen bonds between the valyl amides and the alanyl carbonyl groups with N—O distances of 3.13 Å and 3.20 Å (2.99 Å and 3.33 Å). Although some differences between the individual peptide residues do occur, bond lengths (Table III) and bond angles (Table IV) compare well with those found in most cyclic peptides.¹¹ The

average values are C=O 1.233 Å (1.219 Å), C—N 1.346 Å (1.336 Å), N—C α 1.459 Å (1.432 Å), and C α —C 1.514 Å (1.502 Å). The standard deviation of the bond distances (C—O, C—N, and C—C) range from 0.011 to 0.015 Å (0.016 to 0.025 Å).

The ϕ and ψ conformational angles in the two halves of the TANDEM molecule vary widely, resulting in significant deviations from the symmetric conformation observed for triostin A in solution.¹⁰ The most notable differences are ϕ (L-Val) -102° and -55° (-132° and -106°) and ψ (D-Ser) 16° and -7° (11° and

(11) Karle, I. L.; Gibson, J. W.; Karle, J. J. *Am. Chem. Soc.* **1970**, *92*, 3755-3760. Karle, I. L.; Handa, B. K.; Hassall, C. H. *Acta Crystallogr., Sect. B* **1975**, *B31*, 555-560. Hossain, M. B.; van der Helm, D. J. *Am. Chem. Soc.* **1978**, *100*, 5191-5198.

Table IV. Bond Angles^a

	primed			primed	
N(1)-C(11)-C(12)	114.8 (8)	114.0 (8)	C(41)-C(42)-O(4)	127.7 (9)	127.3 (9)
	117.8 (13)	117.6 (11)		121.0 (17)	124.2 (15)
N(1)-C(11)-C(13)	110.2 (8)	107.3 (7)	C(41)-C(42)-O'(5)	110.8 (8)	109.5 (8)
	109.1 (12)	107.3 (11)		114.9 (14)	111.3 (11)
C(12)-C(11)-C(13)	109.3 (8)	109.3 (8)	O(4)-C(42)-O'(5)	121.0 (9)	122.9 (9)
	109.6 (12)	108.1 (11)		124.1 (18)	124.4 (15)
C(11)-C(12)-O(1)	119.9 (9)	118.1 (8)	C(41)-C(43)-C(44)	109.3 (9)	108.4 (8)
	118.7 (18)	123.3 (12)		125.7 (30)	110.7 (13)
C(11)-C(12)-N(2)	117.1 (8)	117.6 (8)	C(41)-C(43)-C(45)	111.3 (8)	112.2 (8)
	119.1 (15)	115.7 (12)		99.0 (20)	111.2 (12)
O(1)-C(12)-N(2)	122.9 (9)	124.2 (8)	C(44)-C(43)-C(45)	112.5 (9)	111.2 (8)
	122.1 (18)	121.0 (12)		123.1 (34)	114.6 (15)
C(11)-C(13)-O(5)	104.9 (7)	103.6 (7)	C(42)-O(5)-C'(13)	117.4 (7)	117.2 (7)
	106.0 (11)	102.7 (11)		116.6 (13)	116.2 (12)
C(12)-N(2)-C(21)	120.0 (8)	121.3 (7)	C(11)-N(1)-C(101)	119.6 (8)	125.3 (8)
	120.3 (13)	122.4 (11)		118.1 (12)	121.5 (11)
N(2)-C(21)-C(22)	113.0 (8)	108.2 (7)	N(1)-C(101)-O(6)	125.8 (8)	122.1 (8)
	115.6 (13)	110.9 (11)		126.4 (15)	127.7 (14)
N(2)-C(21)-C(23)	107.6 (8)	110.2 (7)	N(1)-C(101)-C(102)	114.0 (8)	114.3 (8)
	108.5 (11)	112.3 (11)		111.3 (12)	110.6 (13)
C(22)-C(21)-C(23)	110.1 (8)	113.3 (8)	O(6)-C(101)-C(102)	120.2 (8)	123.6 (8)
	107.3 (12)	111.2 (12)		122.0 (15)	121.6 (15)
C(21)-C(22)-O(2)	122.3 (8)	123.1 (8)	C(101)-C(102)-C(103)	118.6 (8)	118.9 (8)
	120.9 (13)	115.3 (13)		116.7 (11)	120.3 (15)
C(21)-C(22)-N(3)	116.0 (8)	112.4 (7)	C(101)-C(102)-N(6)	118.0 (8)	119.4 (8)
	116.9 (14)	115.5 (13)		123.4 (14)	115.8 (14)
O(2)-C(22)-N(3)	121.6 (8)	124.4 (8)	C(103)-C(102)-N(6)	123.4 (9)	121.7 (8)
	122.2 (14)	129.1 (14)		119.9 (14)	123.8 (14)
C(22)-N(3)-C(31)	123.9 (8)	122.6 (8)	C(102)-C(103)-N(5)	119.3 (9)	120.5 (9)
	123.5 (13)	122.1 (12)		123.0 (13)	120.4 (15)
N(3)-C(31)-C(32)	108.0 (8)	107.6 (8)	C(103)-N(5)-C(104)	118.1 (8)	119.4 (9)
	109.0 (12)	109.3 (12)		115.2 (12)	122.0 (13)
N(3)-C(31)-C(33)	110.8 (8)	110.0 (8)	N(5)-C(104)-C(105)	116.9 (8)	121.2 (9)
	112.8 (14)	108.7 (11)		118.3 (13)	121.9 (16)
C(32)-C(31)-C(33)	109.7 (8)	111.5 (8)	N(5)-C(104)-C(109)	119.7 (8)	119.4 (8)
	108.5 (13)	109.6 (11)		120.6 (13)	116.9 (14)
C(31)-C(32)-O(3)	121.3 (9)	121.0 (9)	C(105)-C(104)-C(109)	123.4 (9)	119.4 (8)
	124.3 (15)	122.9 (13)		121.1 (15)	121.1 (15)
C(31)-C(32)-N(4)	117.5 (9)	115.6 (9)	C(104)-C(105)-C(106)	117.9 (9)	119.7 (9)
	124.4 (15)	117.5 (12)		120.3 (15)	119.4 (19)
O(3)-C(32)-N(4)	121.2 (10)	123.2 (9)	C(105)-C(106)-C(107)	120.1 (10)	121.8 (9)
	111.3 (15)	119.1 (12)		122.1 (15)	123.6 (20)
C(31)-C(33)-S(1)	116.3 (7)	114.9 (7)	C(106)-C(107)-C(108)	121.9 (10)	119.0 (9)
	115.2 (11)	115.7 (11)		112.6 (16)	119.0 (19)
C(33)-S(1)-S'(1)	105.9 (3)	105.8 (4)	C(107)-C(108)-C(109)	118.2 (9)	121.8 (9)
	105.7 (7)	106.8 (6)		125.9 (16)	116.2 (18)
C(32)-N(4)-C(41)	123.9 (8)	119.3 (8)	C(108)-C(109)-C(104)	118.5 (4)	118.2 (8)
	127.4 (13)	125.8 (11)		118.0 (15)	120.6 (14)
N(4)-C(41)-C(42)	111.7 (8)	111.8 (8)	C(108)-C(109)-N(6)	117.0 (8)	122.0 (9)
	110.8 (13)	108.1 (12)		120.4 (15)	114.3 (15)
N(4)-C(41)-C(43)	111.8 (8)	110.1 (8)	C(104)-C(109)-N(6)	124.5 (9)	119.8 (8)
	109.6 (16)	111.3 (11)		121.6 (14)	125.1 (13)
C(42)-C(41)-C(43)	116.2 (8)	112.5 (8)	C(102)-N(6)-C(109)	115.0 (8)	119.3 (8)
	109.9 (17)	115.1 (12)		119.6 (13)	111.5 (12)

^a Related values in the "unprimed" and "primed" parts of the molecule are listed in parallel columns. Standard deviations are within parentheses.

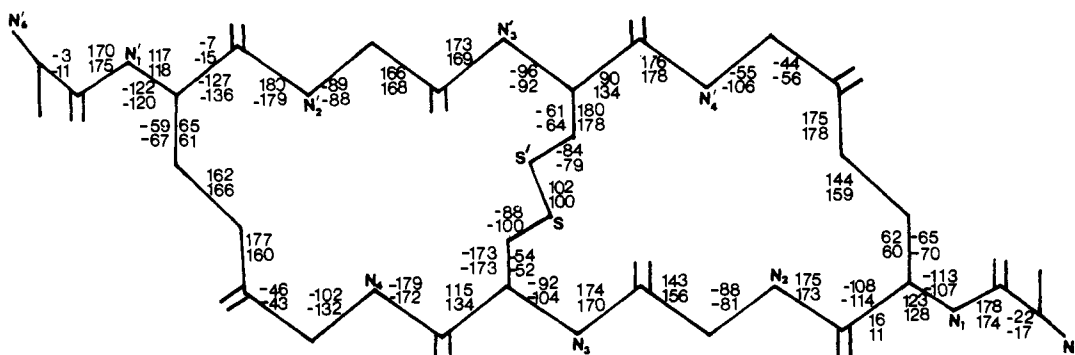


Figure 3. The dihedral angles in the octadepsipeptide. Upper values refer to the LT, lower values to the RT structure.

-15°). The latter affects the relative orientation of the Qxc groups with respect to the peptide ring, introducing further asymmetry

in the molecule. The LT structure appears to be less symmetrical, with $\psi(\text{L-Cys})$ 115° and 90° (both 134°) and $\psi(\text{L-Ala})$ 143° and

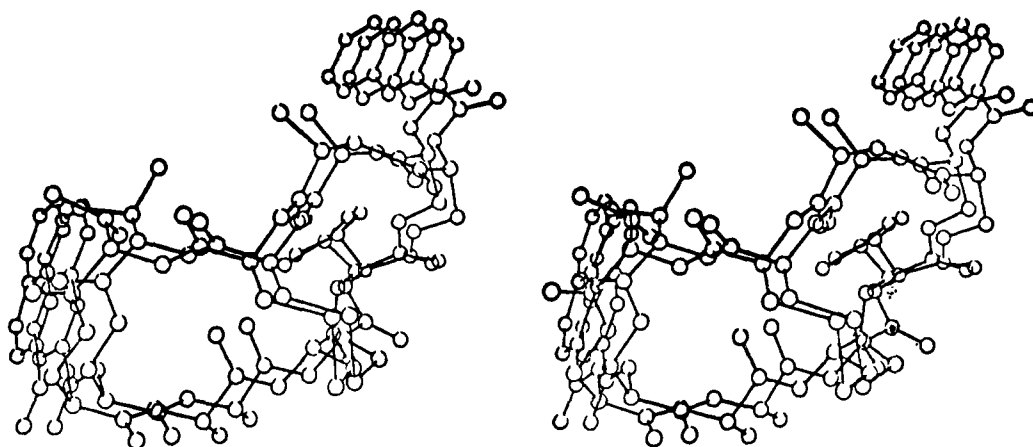


Figure 4. A stereo view of the least-squares fit of the LT and RT structures.

Table V. Hydrogen Bonding Contacts (Å) of the TANDEM Molecules (left) and between the Water Molecules (right)^a

O(1)--W(4)	2.69 (3.36)	W(1)--W(3)	2.83 (2.83)
O(2)--N'(4)	3.13 (2.99)	W(1)--W(7)	2.79 (1.59 ^d)
O(2)--W(3)	2.82 (2.88)	W(2)--W(6)	2.75 (1.76 ^d)
O(3)--W(5)	3.01 (3.03)	W(2)--W(9)	2.86 ^c
O(3)--W(6)	2.97	W(3)--W(12)	2.85
O(4)--W(7)	2.87	W(4)--W(6)	2.81
O(6)--W(2)	3.07	W(4)--W(10)	2.75 (1.27 ^d)
O(6)--W(3)	2.82 (2.89)	W(4)--W(11)	2.84
O'(1)--W(8)	2.98 (3.32)	W(5)--W(6)	2.87 (2.95)
O'(1)--W(10)	2.81 ^b	W(5)--W(14)	2.86 (2.69)
O'(2)--N(4)	3.20 (3.33)	W(6)--W(12)	2.76
O'(6)--W(9)	2.78 (2.77)	W(7)--W(11)	2.75
N(1)--W(1)	2.94 (3.07)	W(7)--W(12)	2.90
N(2)--W(1)	2.83 (2.89)	W(8)--W(11)	2.91
N(3)--W(5)	2.80 (2.86)	W(8)--W(13)	2.74 (1.19 ^d)
N(5)--N'(2)	2.98 (3.12)	W(10)--W(14)	2.71 (2.25 ^d)
N(6)--W(1)	3.03 (3.37)	W(11)--W(14)	2.95
N'(3)--W(9)	2.87 (2.88)	W(12)--W(13)	2.84
N'(5)--W(5)	2.76 (2.82)	W(13)--W(14)	3.00 (2.96)

^a The values for the RT structure are given in parentheses.

^b O'(1)--W(13) 2.74 Å. ^c W(6)--W(9) 2.88 Å. ^d Contacts involving disordered water molecules.

166° (156° and 168°). Contrary to the RT structure, the two ester linkages, both trans, also show significant conformational differences, with torsion angles of 144° and 162°, respectively.

The two Qxc-D-Ser fragments have the same orientation about the trans peptide bond with N-H (D-Ser) pointing up with respect to the peptide ring. The quinoxaline rings are planar within experimental error. However, one carbonyl group is rotated by about 21° (24°) with respect to the aromatic ring, resulting in a displacement of O(6) by 0.46 Å (0.41 Å) from the quinoxaline plane, while O'(6) deviates by only 0.12 Å (0.07 Å).

The disulfide cross-bridge assumes the preferred conformation, but the dihedral angle C-S-S-C of 102° (100°) is somewhat larger than the predicted value (80-90°).¹² There is no indication of a N-H(L-Ala)-O(Qxc) hydrogen bond as suggested for triostin A in solution.¹⁰ The alanyl NH groups are pointing up, whereas the quinoxaline carbonyls are buried inward, leading to N...O distances of 4.59 Å and 4.11 Å (4.62 Å and 4.07 Å).

The drug molecules are completely surrounded by water and there is only one direct interaction between them (Table V). Their environment is quite similar to an aqueous solution, and consequently, the effect of crystal packing forces on the conformation of the molecule should be small. It is noteworthy that in spite of the surfeit of water molecules, one amide [N'(1)] and two carbonyl groups [O'(3) and O'(4)] are not involved in hydrogen bonding at all.

Comparison of the LT and RT Structures. The LT structure is comparatively better refined. The thermal parameters are normal, and the final difference electron-density map was fea-

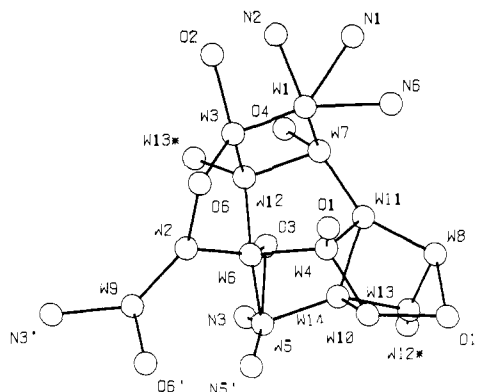


Figure 5. The hydrogen-bonding network at LT formed by the 14 water molecules. ("*" designates symmetry-related atoms).

tureless, with no indication of any disorder or presence of additional solvent atoms. In contrast, the final difference map of the RT structure suggested possible locations of further solvent molecules and indicated partial disorder of one valyl side chain (unprimed atoms).

A stereo view of the least-squares fit of the two structures is given in Figure 4. Although the overall features, including the mode of hydrogen bonding, are quite similar, there are significant conformational differences. The largest deviations occur in the Cys-Val part of the peptide ring, resulting in different intramolecular hydrogen bond lengths and C(11)-C'(11) distances. In addition (see Figure 3), the TANDEM molecule is consistently more symmetrical at RT, while the quinoxaline rings are more parallel in the LT structure.

There are also remarkable differences in the arrangement of the solvent molecules. The LT structure shows two hydration shells consisting of 14 water molecules, which build up a well-ordered network of hydrogen bonds (Figure 5). In the RT structure, the second hydration sphere is replaced by a variety of disordered water and other solvent molecules, whereas the first shell, to a large extent, is still intact. So, although most hydrogen bonds between the water molecules are not present at RT, the intermolecular interactions of TANDEM are almost the same in the two structures (Figure 6).

The following differences between the two structure determinations were observed: the compound was recrystallized from different solvents, the data were taken at different temperatures, and the cell dimensions show significant differences. With respect to the last point, we have observed, as a general rule, a cell volume decrease of 2-3% when crystals are cooled from 20 to -135 °C. In the present case, the difference in the cell volume is 5.5%. This may be caused by the fact that the RT structure, recrystallized from dimethylformamide/ethanol/water, contains more solvent molecules of crystallization. This is possible because not all solvent molecules are located in the RT structure. Even though the first hydration shell is to a large extent the same in both structures,

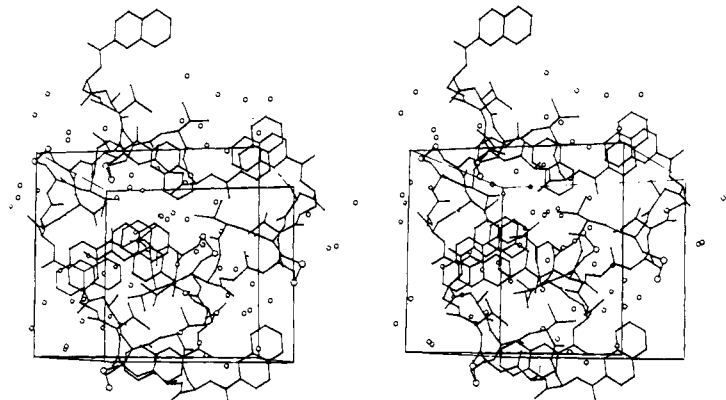


Figure 6. A packing diagram viewed down the *b* axis with *a* horizontal and *c* vertical. The dots indicate water molecules.

Table VI. Effect of a Rotation about the D-Ser C^α-N Bonds on the Distance between the Chromophores in the LT Structure

rotation angle, deg	av distance between the quinoxaline rings, Å	N(2)-O(6), Å	
		Qxc	Qxc'
0	6.5	4.59	4.11
10	8.3	4.45	3.88
20	10.0	4.15	3.62
30	11.4	3.97	3.35
60	13.4	3.15	2.48

both the difference in solvation and the difference in temperature need to be considered as possible causes for the large conformational differences in the two structures. A further distinction can only be made by performing a variable temperature study on the compound.

Discussion

The crystal structure of TANDEM, which consists of a somewhat asymmetric peptide ring with the disulfide cross-bridge lying on the opposite side with respect to the quinoxaline chromophores, is significantly different from the proposed solution structures of triostin A and echinomycin⁹ and that surmised for TANDEM itself.⁸ Although the two points of attachment of the chromophores are separated by 11.9 Å (12.2 Å), the perpendicular distance between the quinoxaline rings is only about 6.5 Å. It is obvious that the drug molecule in its solid-state conformation cannot participate in two-base-pair-sandwich intercalation. Thus, the relative orientation of the Qxc groups must be changed in order to achieve a separation of about 10 Å to allow for the accommodation of two base pairs in the intercalated complex with DNA. The D-Ser C^α-N bonds outside the peptide ring are expected to enjoy considerable conformational flexibility, as is the case in linear peptides.^{9,13} Such flexibility would permit variation in the separation distance of the two chromophores and would also change the relative disposition of the Qxc groups and the L-Ala amide groups. Table VI shows that a rotation of about 20° gives the desired 10-Å separation. Therefore, the two Qxc groups have to be rotated by unequal amounts due to molecular asymmetry. The maximum separation of about 13 Å require rotation by about 60°, which would, however, lead to short N(2)-O(6) contacts. Using such a modified conformation, it is possible to not only construct

a model of an intercalated complex between TANDEM and B-DNA, but also account for the known specificity of this drug in alternating adenine-thymine sequences.¹⁴

The presence of the disulfide cross-bridge and the two intramolecular N-H...O hydrogen bonds linking the antiparallel peptide chains suggests that the peptide ring is fairly rigid. The surprisingly large conformational differences between the LT and RT structures show, however, that it can undergo significant conformational changes. The orientations of some carbonyl groups, in particular, seem to be affected by hydrogen-bonding interactions with the surrounding water network, which, as discussed above, is rather different in the two crystal structures.

Although TANDEM and triostin A are closely related, it is rather speculative to extrapolate from the present crystal structure to the detailed conformation of the natural antibiotic. The N-methylated L-Val residues in triostin A not only preclude the formation of the intramolecular N-H...O hydrogen bonds observed in TANDEM but must also cause significant conformational changes because of steric hindrance between the methyl and carbonyl groups. Therefore, triostin A is expected to have a somewhat more flexible peptide backbone, which could be the reason for its different binding properties to DNA as compared to TANDEM. So, in addition to a detailed model for TANDEM, the present crystal structure has given some new insight into the conformational behavior of the related antibiotics and how they might interact with DNA.

Acknowledgment. The group at Cambridge thanks the MRC for financial support, the SRC for the diffractometer, the Deutsche Forschungsgemeinschaft for a postdoctoral fellowship (E.E.), and Dr. W. B. T. Cruse for helpful discussion. M.A.V. thanks the Department of Science and Technology, India, for financial support. The research in Oklahoma was sponsored by a grant from National Institute of General Medical Science (GM 21822) and a grant from the National Cancer Institute, DHEW (CA-17562).

Registry No. TANDEM, 63478-55-7.

Supplementary Material Available: Final thermal parameters and structure factors (38 pages). Ordering information is given on any current masthead page.

(13) Ughetto, G.; Waring, M. J. *Mol. Pharmacol.* **1977**, *13*, 579-584.

(14) Viswamitra, M. A.; Kennard, O.; Cruse, W. B. T.; Egert, E.; Sheldrick, G. M.; Jones, P. G.; Waring, M. J.; Wakelin, L. P. G.; Olsen, R. K. *Nature (London)* **1981**, *289*, 817-819.